

Electronic Supporting Information

High and reversible SO₂ capture by a chemically stable Cr(III)-based MOF

Eva Martínez-Ahumada,^{†a} Mariana L. Díaz-Ramírez,^{†a} Hugo A. Lara-García,^b Daryl R. Williams,^c Vladimir Martis,^d Vojtech Jancik,^{e,f} Enrique Lima^{*,a} and Ilich A. Ibarra^{*,a}

^a *Laboratorio de Fisicoquímica y Reactividad de Superficies (LaFReS), Instituto de Investigaciones en Materiales, Universidad Nacional Autónoma de México, Circuito Exterior s/n, CU, Coyoacán, 04510, Ciudad de México, México.*

^b *Instituto de Física, Universidad Nacional Autónoma de México, Circuito de la Investigación Científica s/n, CU, Coyoacán, Ciudad de México, México.*

^c *Surfaces and Particle Engineering Laboratory (SPEL), Department of Chemical Engineering, Imperial College London, South Kensington Campus, London SW7 2AZ, UK.*

^d *Surface Measurement Systems, Unit 5, Wharfside, Rosemont Road, London HA0 4PE, UK.*

^e *Universidad Nacional Autónoma de México, Instituto de Química, Ciudad Universitaria, Ciudad de México, 04510, México.*

^f *Centro Conjunto de Investigación en Química Sustentable UAEM-UNAM, Carr. Toluca-Atlacomulco Km 14.5, Toluca, Estado de México 50200, México. Personal del Instituto de Química de la UNAM*

Table of Contents

S1. Experimental Details	3
S2. Bulk Powder XRD	4
S3. Thermogravimetric Analysis	6
S4. Adsorption Isotherms of N₂ and SO₂	7
S5. Isosteric Heat of Adsorption of SO₂	10
S6. DRIFTS	12
S7. Homemade Wet SO₂ Adsorption Experiment Set Up	13
S8. Other Fluorinated Samples	15
S9. MIL-101(Cr) SO₂ Adsorption	17
S11. Additional characterization for MIL-101(Cr)-4F(1%)	21
S10. References	22

Experimental Section

S1. Experimental Details

Material synthesis

MIL-101(Cr)-4F(1%). MIL-101(Cr)-4F(1%) was synthesised adapting the synthetic methods previously reported by Kitagawa and co-workers and Lima *et al.*^{1a,1b} CrO₃ (12 mmol), H₂BDC (8.75 mmol), H₂BDC-4F (3.75 mmol) and concentrated aqueous hydrochloric acid (12.5 mmol) were mixed in water (50 mL). The resulting suspension was heated to 473 K for 6 days in a Teflon-lined autoclave under autogenous pressure. As we previously reported,^{1b} the mother liquor and the solid formed were separated by filtration. The mother liquor was analysed by UV/vis looking for unreacted ligands and only H₂BDC-4F was found. This result is consistent since H₂BDC-4F is fairly soluble in water even at low pH (approximately 11 mg/mL), while H₂BDC is not water-soluble. The recovered solid, comprising the MOF material (MIL-101(Cr)-4F(1%)) and unreacted ligand, was washed (five times) with NaOH (0.8 M) and the pure MOF material was separated by filtration. This recovered material was then washed (five times) with water to remove any excess of NaOH (0.8 M). Interestingly, the rinsing with NaOH led to the replacement of the Cl⁻ anion for HO⁻, as confirmed by elemental analysis. An activated sample of MIL-101(Cr)-4F(1%) (acetone-exchanged and 453 K for 2 h under vacuum; 10⁻⁶ bar) was analysed by elemental analysis (average data from five independent experiments, see Table S1), corresponding to [Cr₃O(BDC)_{2.91}(BDC-F₄)_{0.09}]-OH: calcd (%) for $M_T = 687.8$ g/mol C 41.90; H 1.80; F 0.98; found: C 41.91; H 1.85; F 0.99%.

Table S1. Elemental analysis data for MIL-101(Cr)-4F(1%) activated sample [Cr₃O(BDC)_{2.91}(BDC-F₄)_{0.09}]-OH.

Element	Calculated	Run					Average
		1	2	3	4	5	
C	41.9	42.02	42.18	42.34	42.63	42.22	42.28
H	1.85	1.89	1.9	1.84	1.9	1.86	1.878
F	0.99	0.99	0.98	1.01	0.97	0.98	0.986
BDC-F4/BDC ratio	1/33.4	1/33.5	1/34.0	1/33.1	1/34.7	1/34.0	1/33.9

Sample activation

Before the adsorption experiments, the samples were acetone-exchanged to remove any uncoordinated solvents (water and DMF) from the pores. These samples were activated at 453 K for 2 h (with a heating ramp of 5 K min⁻¹) under vacuum (10⁻⁶ bar) to afford the fully desolvated samples.

S2. Bulk Powder XRD

Powder X-Ray Diffraction Patterns (PXRD) were collected on a Rigaku Diffractometer, Ultima IV with a Cu-K α_1 radiation ($\lambda = 1.5406 \text{ \AA}$) using a nickel filter. Patterns were recorded in the 2–25° 2 θ range with a step scan of 0.02° and a scan rate of 0.08° min⁻¹.

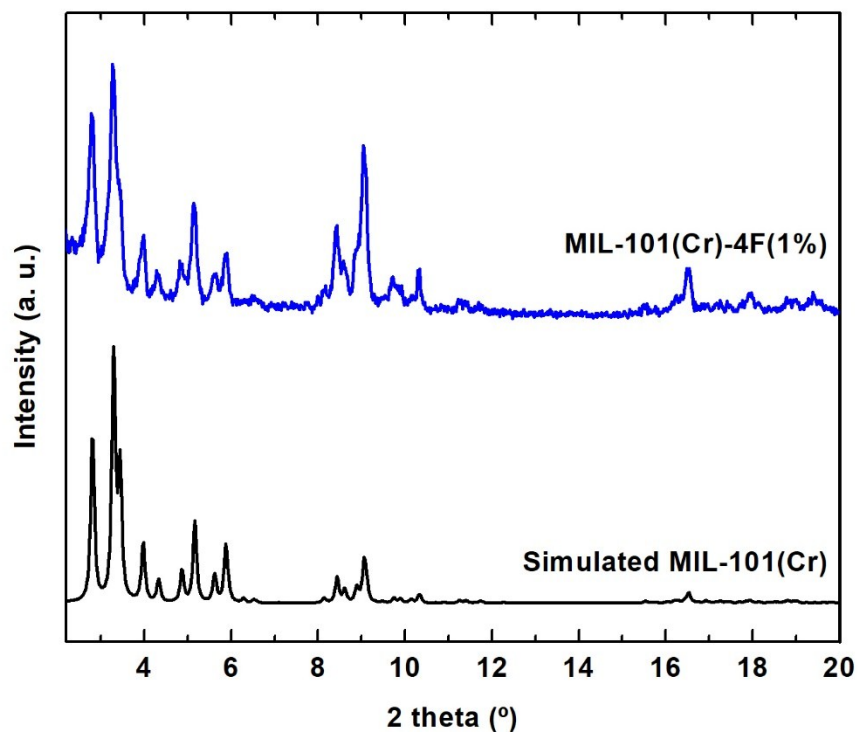


Fig. S1. PXRD patterns of MIL-101(Cr)-4F(1%) as synthesised.

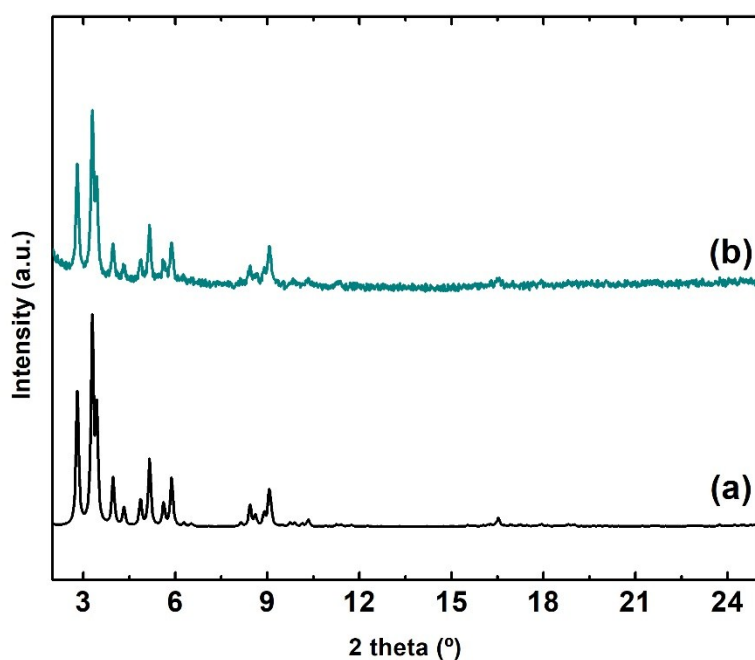


Fig. S2. PXRD patterns of (a) simulated MIL-101(Cr) and (b) MIL-101(Cr)-4F(1%) after SO₂ adsorption.

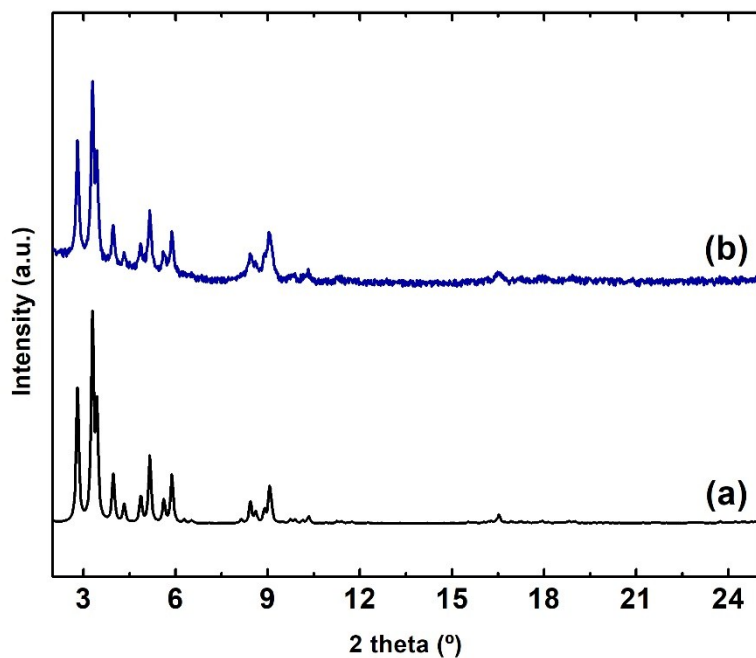


Fig. S3. PXRD patterns of (a) simulated MIL-101(Cr) and (b) MIL-101(Cr)-4F(1%) after 50 SO₂ adsorption/desorption cycles.

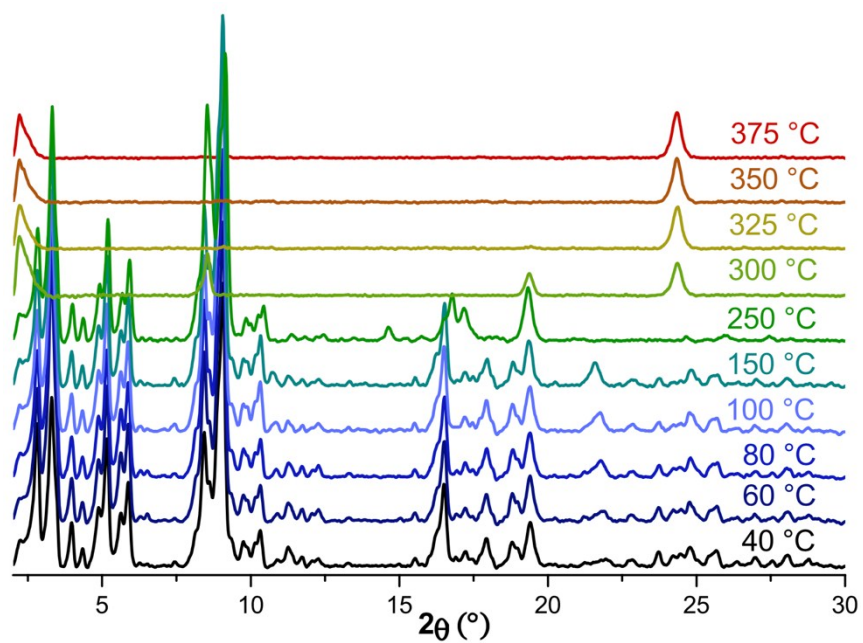


Fig. S4. *In situ* PXRD patterns of SO₂ re-cycled MIL-101(Cr)-4F(1%) up to 648 K (375 °C).

S3. Thermogravimetric Analysis

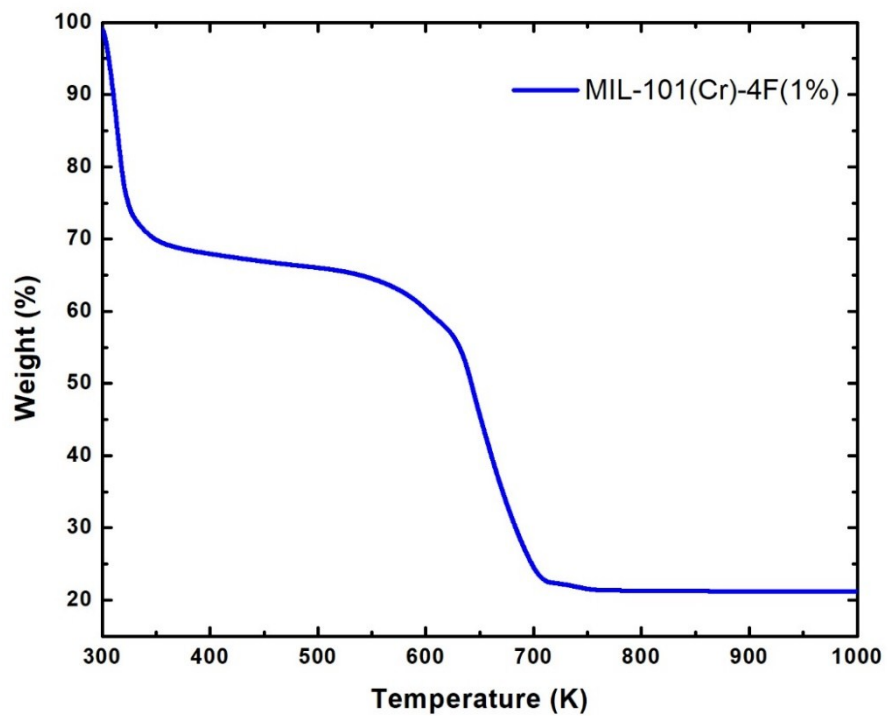


Fig. S5. TGA trace of as synthesised MIL-101(Cr)-4F(1%).

S4. Adsorption Isotherms of N₂ and SO₂

N₂ isotherms (up to $P/P_0 = 1$ and 77 K) were recorded on a Quantachrome Autosorb MP-1 equipment under high vacuum in a clean system with a diaphragm pumping system. SO₂ isotherms were recorded at 298 K and up to 1 bar with the aid of a Dynamic Gravimetric Gas/Vapour Sorption Analyser, DVS Vacuum (Surface Measurements Systems Ltd.). Ultra-pure grade (99.9995%) N₂ and SO₂ were purchased from PRAXAIR.

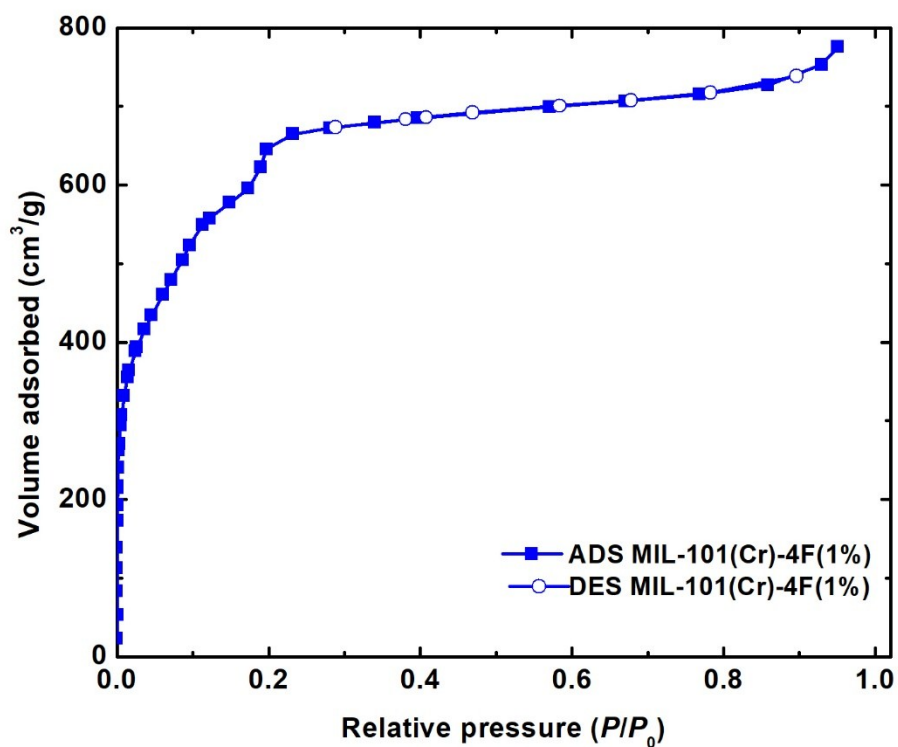


Fig. S6. N₂ adsorption isotherm at 77 K of as synthesized MIL-101(Cr)-4F(1%).

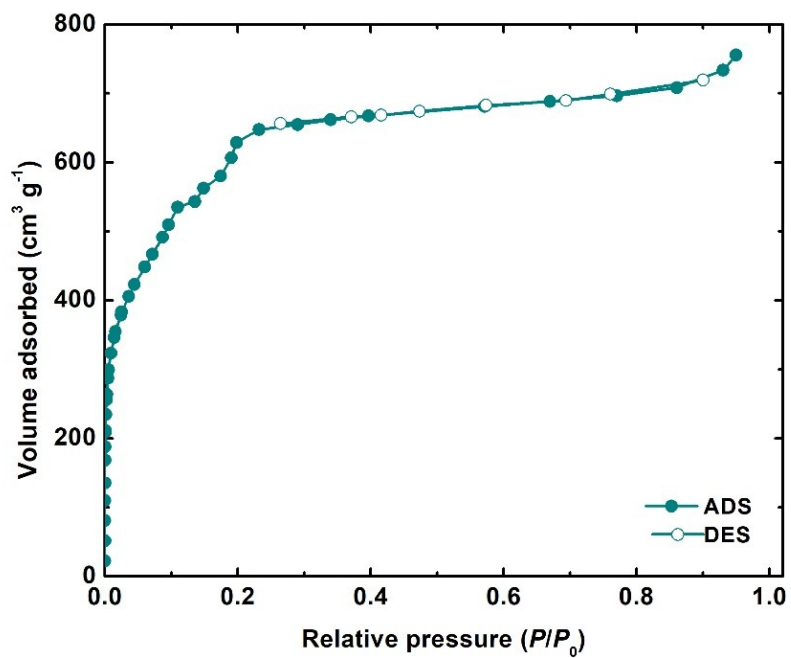


Fig. S7. N_2 adsorption isotherm at 77 K of MIL-101(Cr)-4F(1%) after SO_2 adsorption.

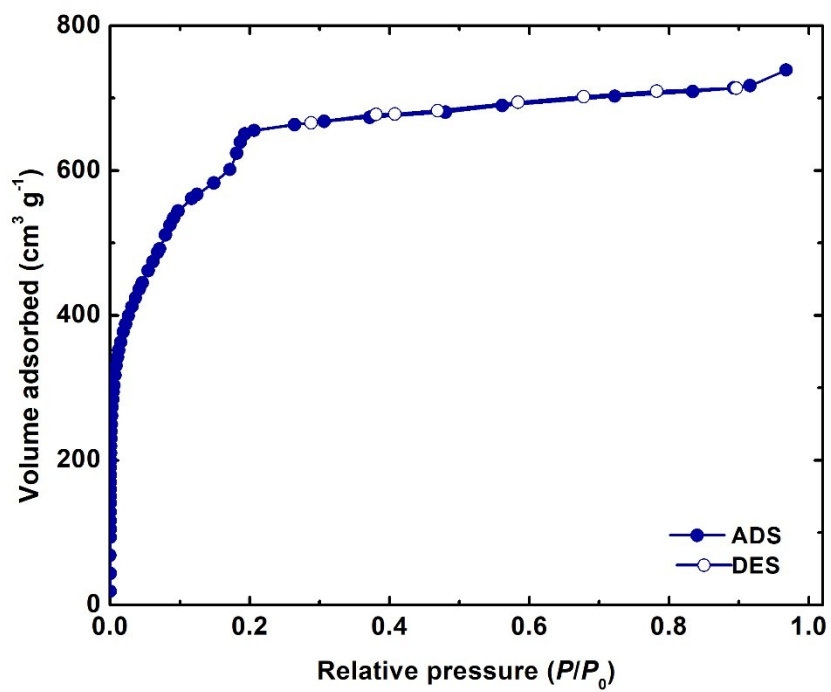


Fig. S8. N_2 adsorption isotherm at 77 K of MIL-101(Cr)-4F(1%) after 50 SO_2 adsorption/desorption cycles.

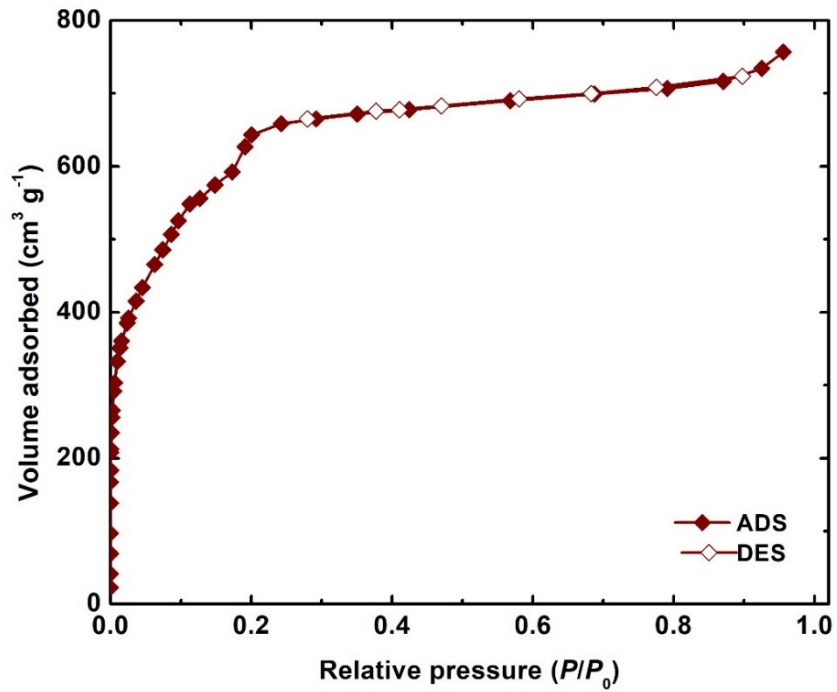


Fig. S9. N_2 adsorption isotherm at 77 K of MIL-101(Cr)-4F(1%) after $\text{SO}_2/\text{H}_2\text{O}$ exposure.

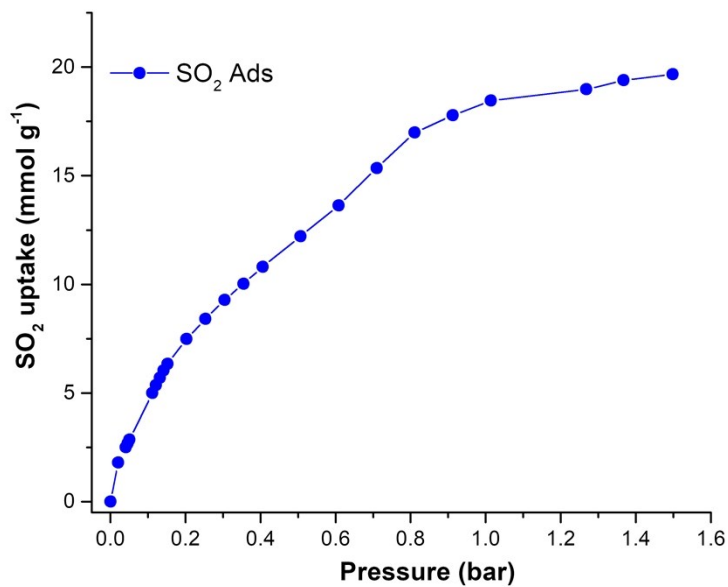


Fig. S10. SO_2 adsorption isotherm of MIL-101(Cr)-4F(1%) at 298 K and 1.5 bar.

S5. Isotheric Heat of Adsorption of SO₂

The heat of adsorption of SO₂, ΔH , was calculated by the isotheric method for the MIL-101(Cr)-4F(1%), using the corresponding adsorption isotherms at three different temperatures (Fig. S11A, C, E). A virial-type equation was used to fit the adsorption isotherms:

$$\ln\left(\frac{n}{p}\right) = A_0 + A_1n + A_2n^2 + \dots \quad \text{Eq. S5.1}$$

where p is the pressure, n is the amount adsorbed and A_0, A_1, \dots are the virial coefficients (A_2 and higher terms can be ignored at lower coverage values). A plot of $\ln(n/p)$ versus n should give a straight line at low surface coverage (Fig. S11B, D, F).

The obtained values and their average ($-54.3 \text{ kJ mol}^{-1}$) are reported on Table S2.

Table S2. Calculated heats of adsorption at three different temperatures 298, 303 and 308 K.

T [K]	Calculated Q _{st} [kJ mol ⁻¹]
298 and 303	-52.66
303 and 308	-57.40
298 and 308	-52.95
Average=	-54.34

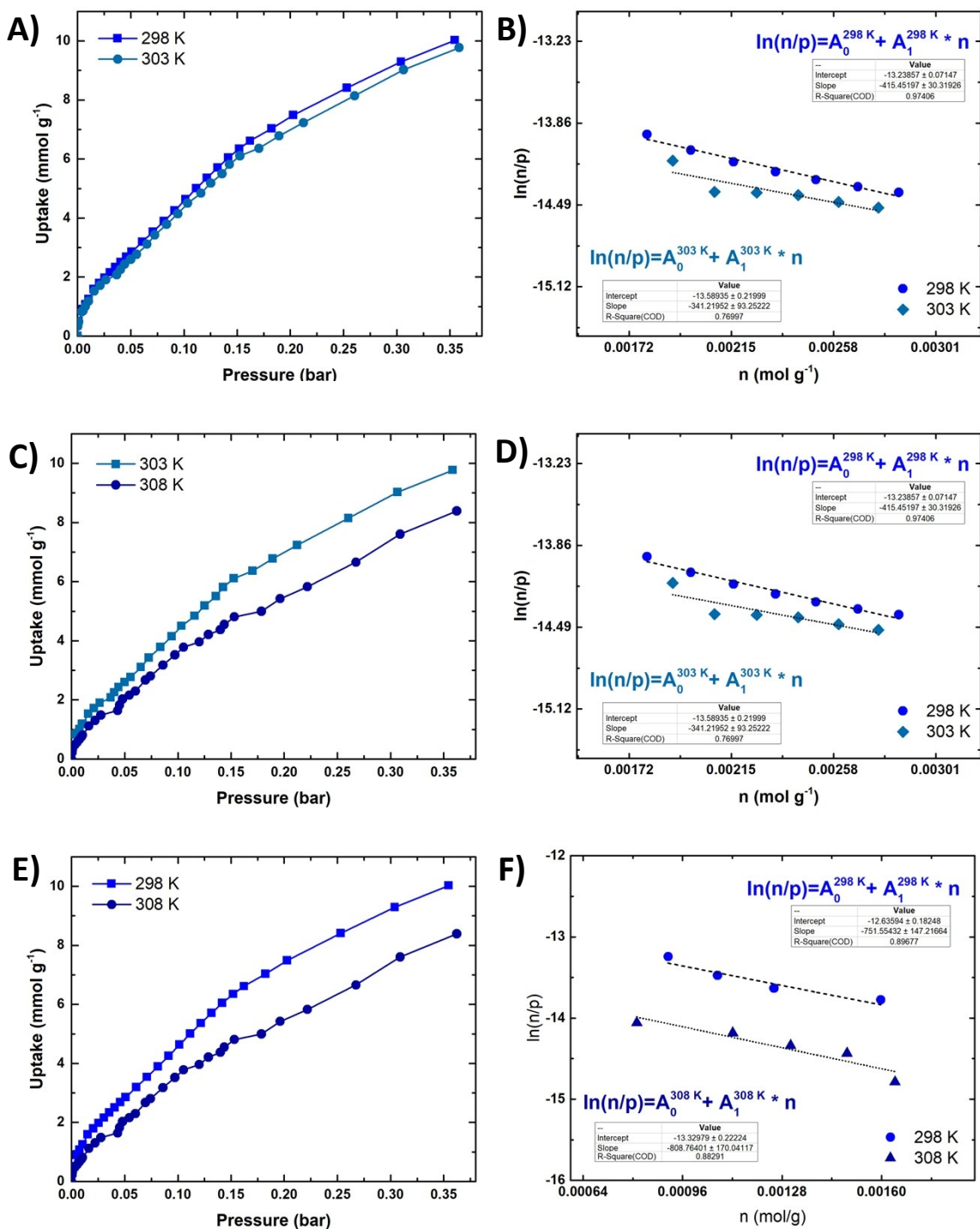


Fig. S11. SO₂ adsorption isotherms at A) 298 and 303 K, C) 303 and 308 K, E) 298 and 308 K, for MIL-101(Cr)-4F(1%). Virial fitting plots at B) 298 and 303 K, D) 303 and 308 K, F) 298 and 308 K.

S6. DRIFTS

DRIFTS experiments were performed using an environmentally controlled PIKE DRIFTS cell with ZnSe windows coupled to a Thermo Scientific Nicolet iS50 spectrometer with a MCT/A detector. Absorbance spectra were obtained by collecting 64 scans at a 4 cm^{-1} resolution. A sample of 0.020 g was pre-treated in situ under a N_2 flow at 453 K for 3 h. After this treatment, the sample was cooled to room temperature and then, a flow of carbon monoxide (CO: 30 mL/min; 5 % of CO diluted in He) was passed through the sample. Spectra of the solid were collected every 10 min.

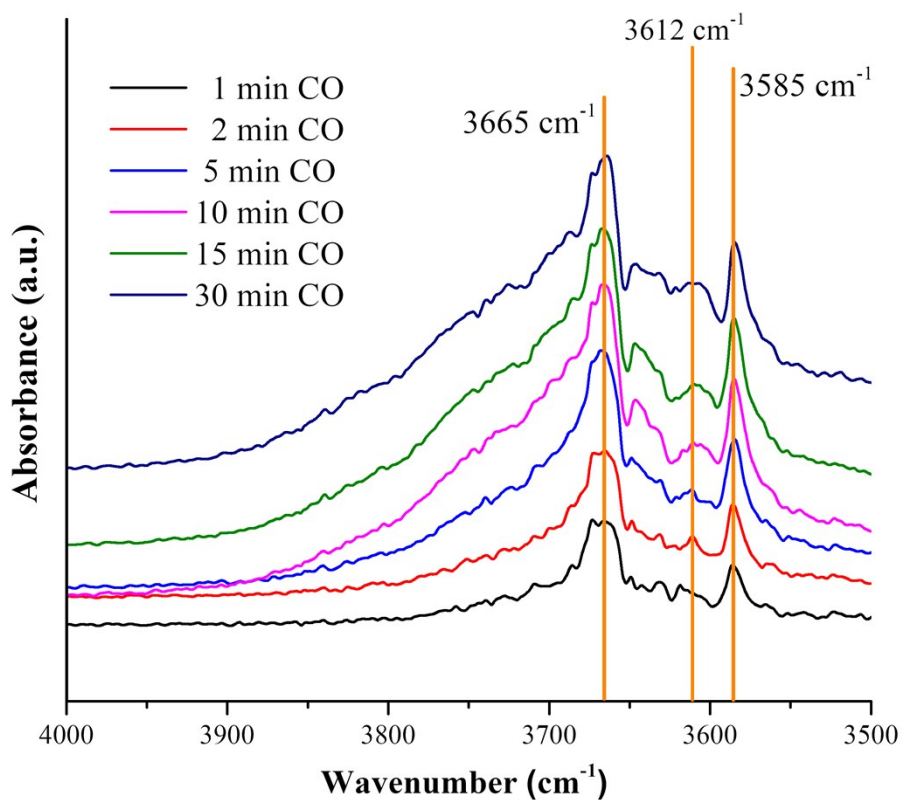


Fig. S12. DRIFT spectra of CO adsorption on MIL-101(Cr)-4F(1%) from $\tilde{\nu}$ 4000 to 3500 cm^{-1}

S7. Homemade Wet SO₂ Adsorption Experiments

The system adapted from the reported literature.² The system contains two principal parts: SO₂ gas generator (A) dropping funnel with H₂SO₄ conc. [1] connected to a schlenk flask with Na₂SO₃ (s) under stirring [2]; and the saturation chamber (B), constructed from a round flask with distilled water [3], connected to a sintered glass filter adapter [4] and to a vacuum line [5]. The activated sample is placed on the glass filter adapter.

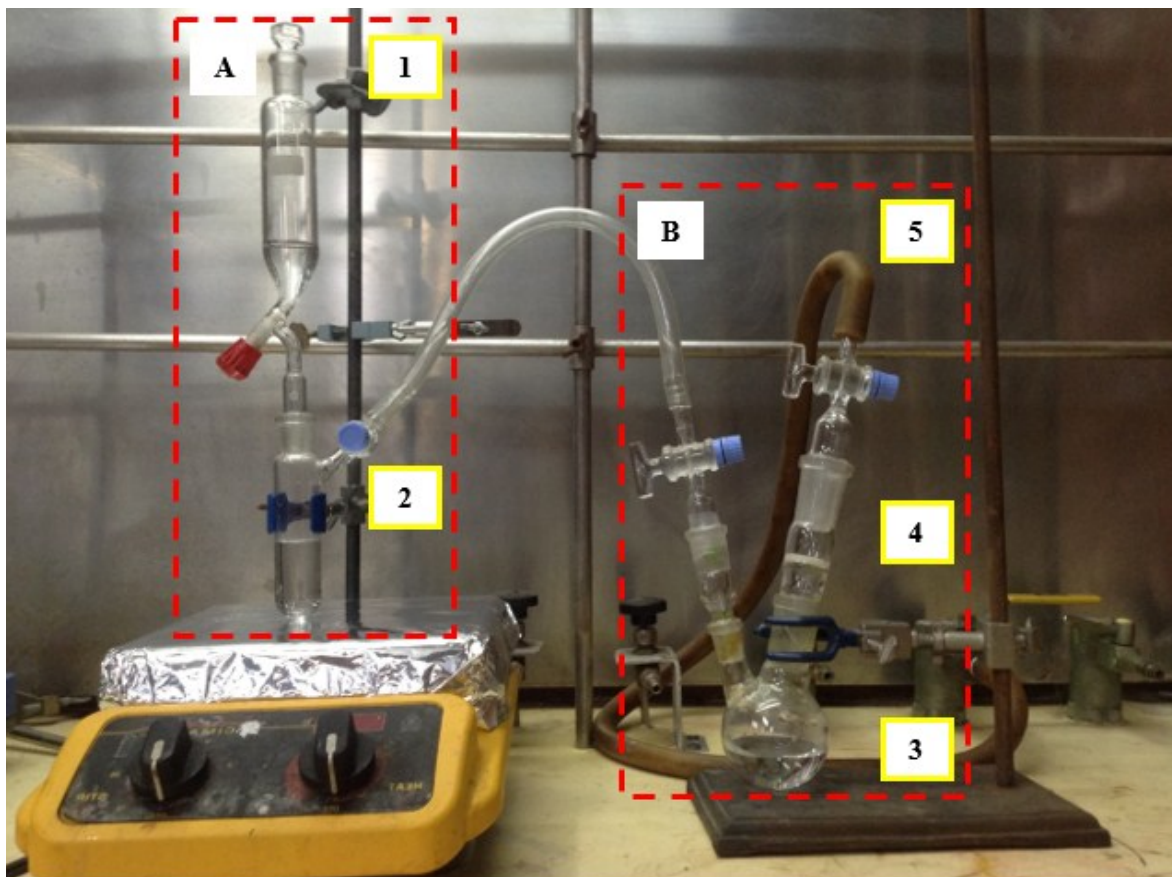


Fig. S13. Homemade system for wet SO₂ adsorption experiments.

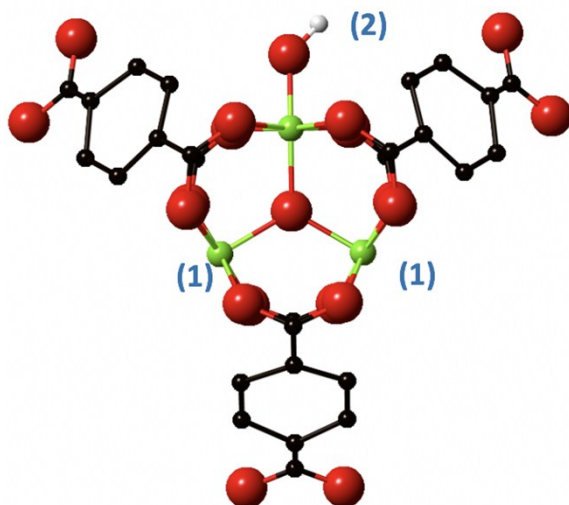


Fig. S14. Representation of the activated trinuclear building block of MIL-101(Cr)-4F(1%) showing the preferential adsorption sites: (1) Lewis acid sites (open metal sites); (2) Brønsted acid sites (hydrogen atom of the HO group).

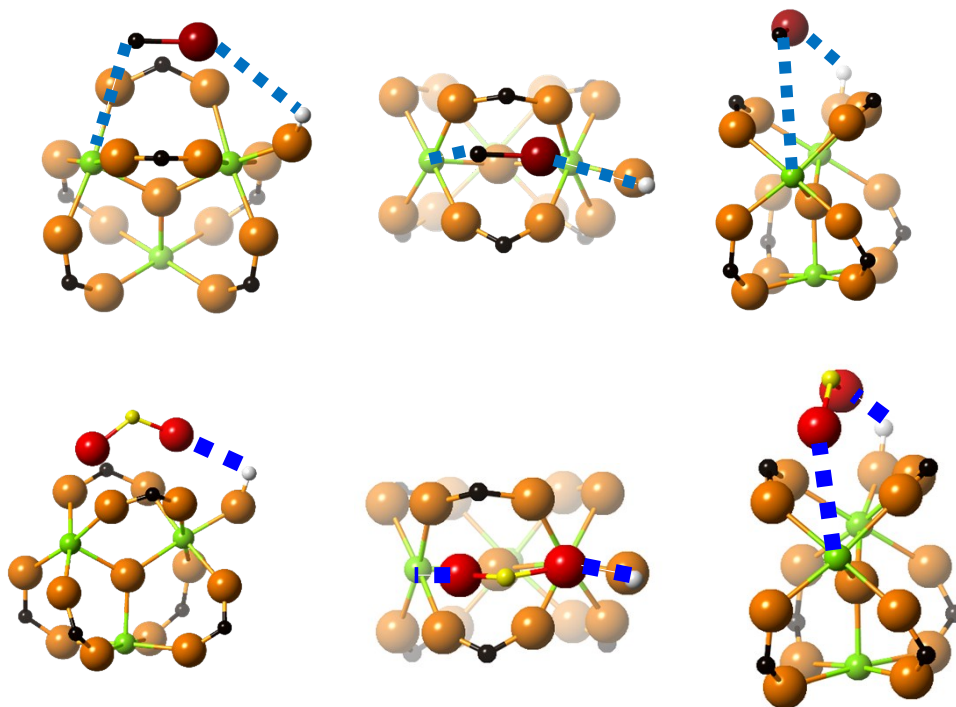


Fig. S15. (top) schematisation of the interaction between CO and the trimeric cluster of MIL-101(Cr)-4F(1%) from different perspectives; (bottom) schematisation of the interaction between SO₂ and the trimeric cluster of MIL-101(Cr)-4F(1%) from different perspectives. Orange: oxygen from the cluster; red: oxygen from CO and SO₂; black: carbon, green: chromium, yellow: sulphur, dotted blue lines represent electrostatic interactions. For purposes of clarity and a better visualisation, the linkers have been removed.

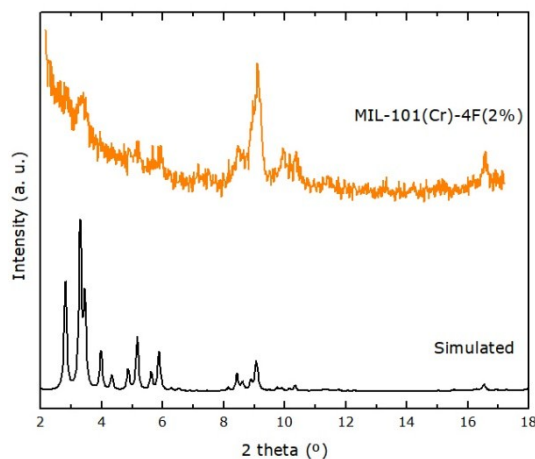
S8. Other Fluorinated Samples

Using the previously described method (vide supra), we attempted to synthesize fluorinated samples of MIL-101(Cr) with varying fluorine content. However only two resulted in crystalline samples (Table S3).

Table S3. Synthetic tests for MIL-101(Cr) with different fluorinated linker amounts.

Target fluorine content	Crystalline
1%	Yes
2%	Yes
5%	No
10%	No
50%	No

A brief characterization is presented below. As can be seen, PXRD confirms the MIL-101(Cr) phase (Fig. S14),



however, the sample presents a reduced BET surface area ($1310 \text{ m}^2 \text{ g}^{-1}$, see Fig. S15).

Fig. S16. PXRD patterns of (a) simulated MIL-101(Cr) and (b) as-synthesized MIL-101(Cr)-4F(2%).

Table S4. Elemental analysis data for MIL-101(Cr)-4F(2%) activated sample $[\text{Cr}_3\text{O}(\text{BDC})_{2.91}(\text{BDC}-\text{F}_4)_{0.19}]\cdot\text{OH}$.

Element	Calculated	Run					Average
		1	2	3	4	5	
C	41.19	41.24	41.49	41.03	41.06	41.36	41.23
H	1.62	1.79	1.36	1.25	1.68	1.75	1.57
F	2.00	2.15	2.01	2.09	1.99	2.00	2.05

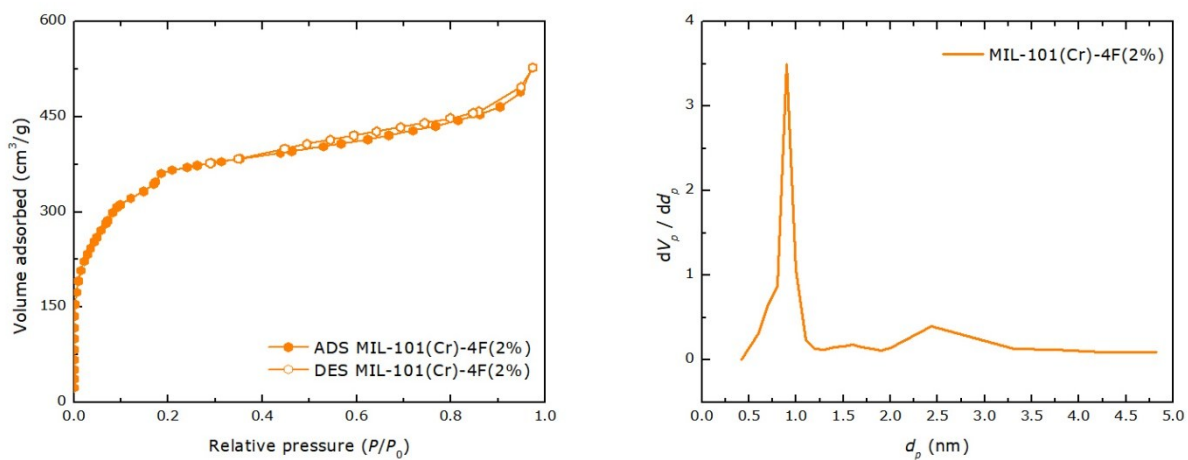


Fig. S17. N₂ adsorption isotherm at 77 K of as synthesized MIL-101(Cr)-4F(2%) and pore distribution plot.

S9. MIL-101(Cr) SO₂ Adsorption

MIL-101(Cr) was synthesised adapting the synthetic methods previously reported by Lima *et al.*^{1b} Cr(NO₃)₃·9H₂O (10 mmol), H₂BDC (10 mmol) were mixed in water (50 mL). The resulting suspension was heated to 473 K for 8 hours in a Teflon-lined autoclave under autogenous pressure. After the synthesis was finished, the product was recovered by filtration and then washed with DMF and then, acetone-exchanged. PXRD confirmed phase purity. Following the same activation steps for MIL-101(Cr)-4F(1%), 180 °C during 3 h under vacuum, we measured a SO₂ isotherm at 298 K for MIL-101(Cr). The maximum uptake at this temperature was 16.0 mmol g⁻¹, at 1 bar (Fig. S18). As shown in Fig. S19B, crystallinity was not retained after SO₂ adsorption-desorption experiment.

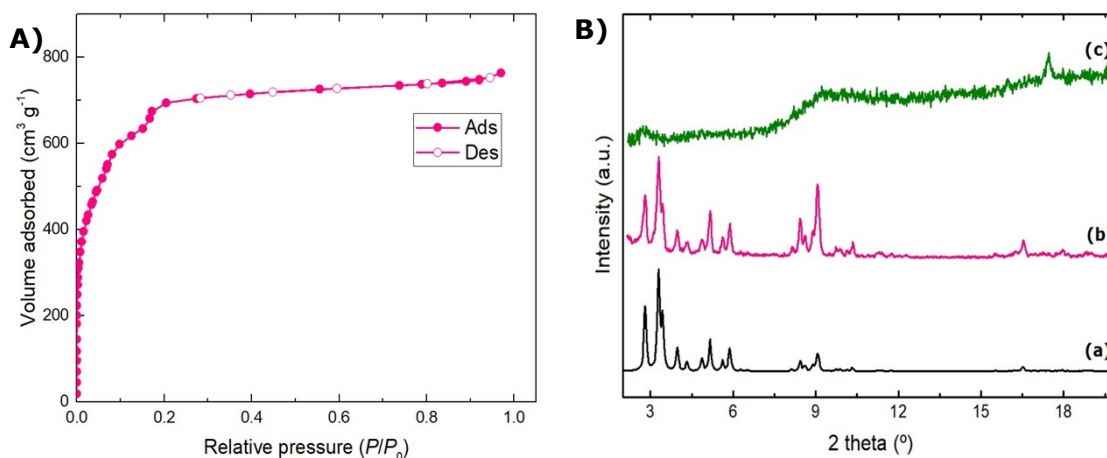
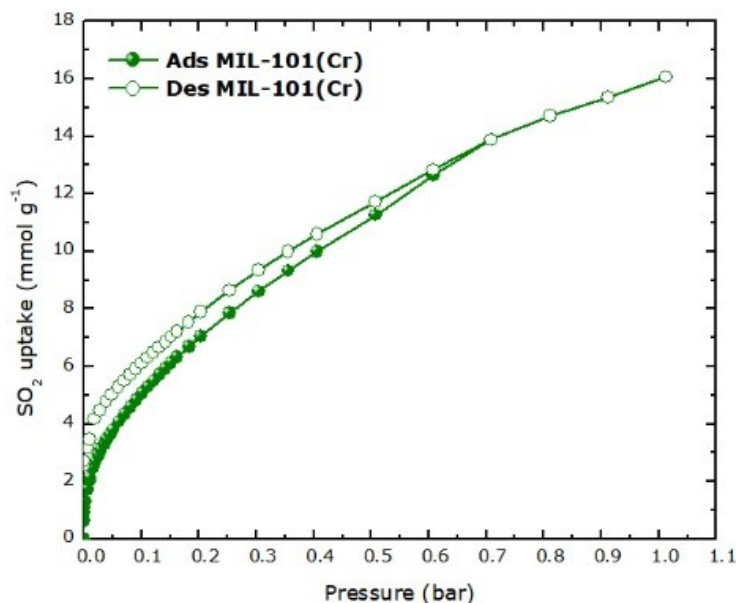


Fig. S18. SO₂ adsorption isotherm at 298 K for MIL-101(Cr).

Fig. S19. A) N₂ isotherm at 77 K for as synthesized MIL-101(Cr) and B) PXRD patterns of MIL-101(Cr): (a) simulated, (b) as-synthesized and (c) after the SO₂ adsorption isotherm.

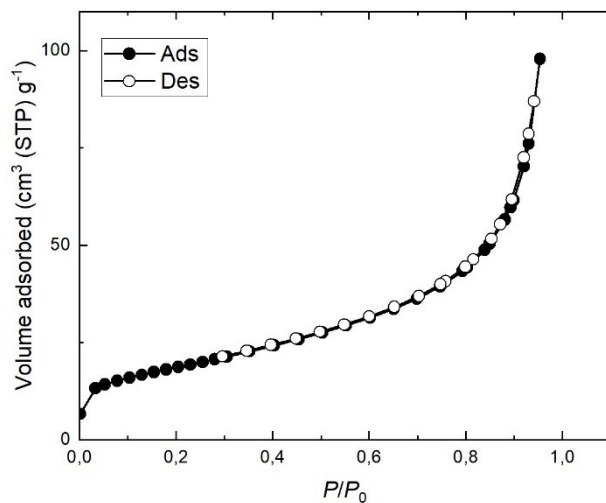


Fig. S20. N₂ adsorption isotherm at 77 K of MIL-101(Cr) after the SO₂ adsorption experiment.

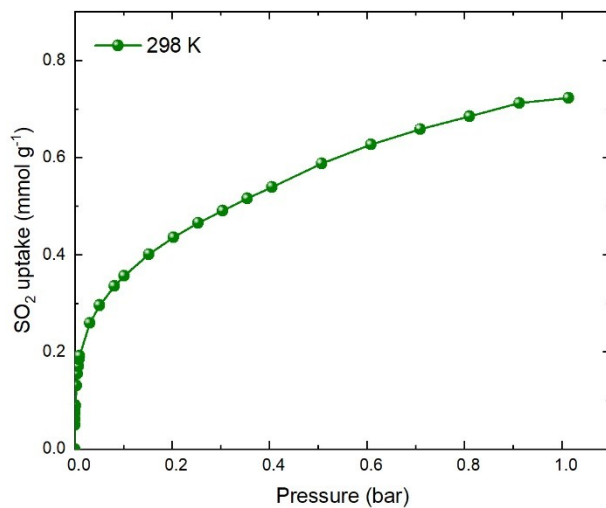


Fig. S21. Second SO₂ adsorption isotherm at 298 K for MIL-101(Cr).

MIL-101(Cr) synthesised with HF: MIL-101(Cr)-HF

Another MIL-101(Cr) synthesis was performed following a reported methodology.⁴ Concisely, 1.6 g of terephthalic acid (H₂BDC), 4 g of Cr(NO₃)₃·9H₂O and 200 μL of HF were mixed in 50 mL of distilled water. The mixture was heated up to 493 K during 8 h in a Teflon-lined autoclave under autogenous pressure. The product was filtered and then washed with dimethylformamide and then, acetone-exchanged. The sample was named **MIL-101(Cr)-HF**. PXRD was carried out to confirm MIL-101(Cr) structure (see **Fig. S22**) and N₂ physisorption at 77 K (Fig. S23) was measured to estimate the BET surface area, which resulted to be: 3188 m² g⁻¹. SO₂ isotherms were performed at 298 K as described in section S4, resulting isotherms are shown in Fig. S24. Maximum uptake for the first isotherm was 20.3 mmol SO₂ g⁻¹ at 298 K an up to 1 bar. As the crystal structure after this first run has not completely collapsed (see **Fig. S22**), we performed a second adsorption-desorption isotherm at the same temperature. However, this second measurement resulted in less than the half (9.8 mmol SO₂ g⁻¹) of the previously SO₂ uptake exhibited by the same material.

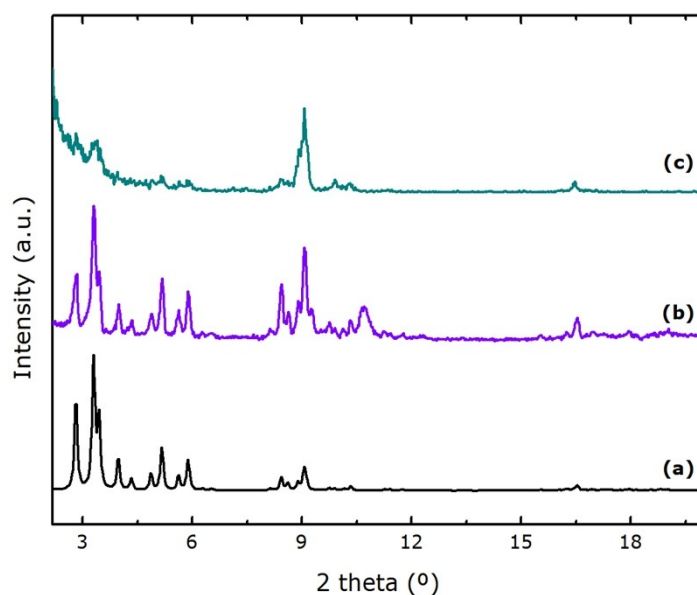


Fig. S22. PXRD patterns of (a) simulated, (b) as-synthesised and (c) after SO₂ exposure of MIL-101(Cr)-HF.

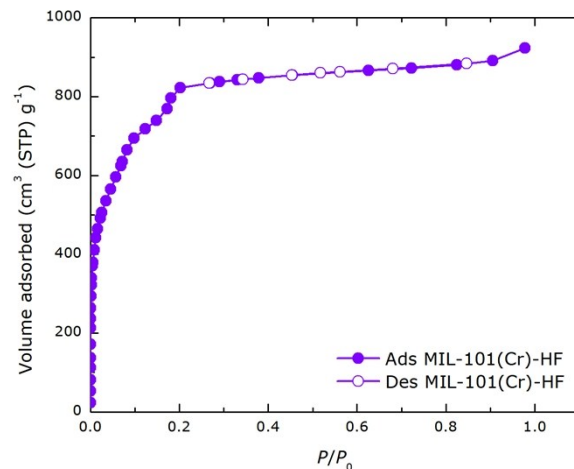


Fig. S23 N₂ isotherm at 77 K for as-synthesised MIL-101(Cr)-HF.

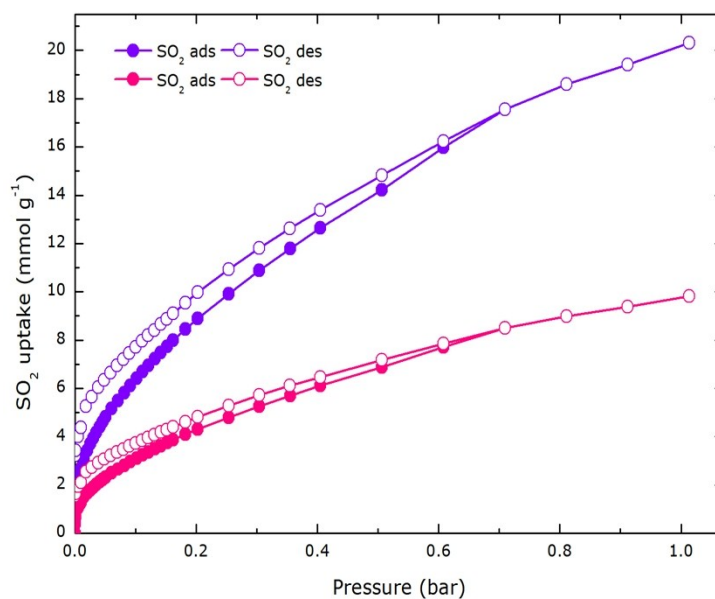


Fig. S24. SO₂ isotherms for MIL-101(Cr)-HF at 298 K and up to 1 bar. Violet line, first measurement, Pink line, second measurement.

S11. Additional Characterization for MIL-101(Cr)-4F(1%)

^{19}F MAS NMR spectra were measured in a Bruker Avance 300 spectrometer at a Larmor frequency of 376.3 MHz, using $\pi/2$ pulses of 6 ms with a recycle delay of 1 s; ^{19}F chemical shifts were referenced to those of CFCl_3 at 0 ppm.

The spectra support the incorporation of fluorinated ligand to the MOF material. The difference in the signal/noise ratio and the number of scans (100 for spectrum of the fluorinated ligand and 10,000 for the spectrum of MIL-101(Cr)-4F(1%)) supports the very low-content fluorine in MIL-101(Cr)-4F(1%). The broader peaks in the spectrum of MIL-101(Cr)-4F(1%) are in good correlation with a homogeneous spread of the chemical shift which is consistent with the dispersion of the fluorinated ligand within MIL-101(Cr)-4F(1%).

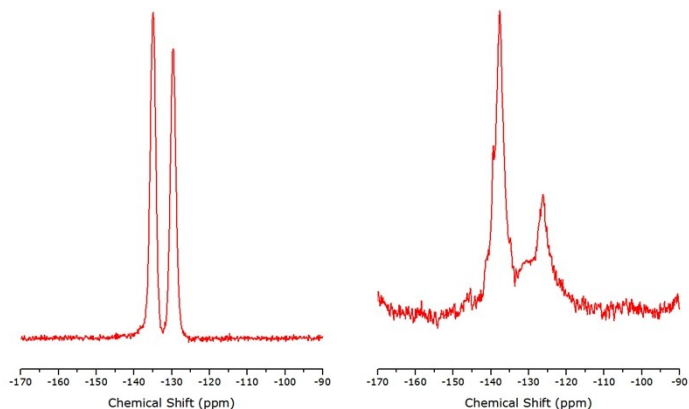


Fig. S25. Solid State (MAS) NMR ^{19}F spectra of the fluorinated ligand (left) and MIL-101(Cr)-4F(1%) (right).

X-ray photoelectron spectroscopy (XPS) studies were performed using a JEOL JPS 9010 MC photoelectron spectrometer, using Mg $K\alpha$ (1253.6 eV) radiation from an X-ray source operating at 10 kV and 20 mA, and the base pressure in the analysis was kept in the range from 5×10^{-10} to 1×10^{-9} mbar.

F 1s XPS spectrum of MIL-101(Cr)-4F(1%) showing only one signal at 688.5 eV which irrefutably demonstrates the presence of organic fluorine C-F as earlier reported by Zhang et al.⁵ The intensity of the signal is very weak consistent with the very low amount of fluorine.

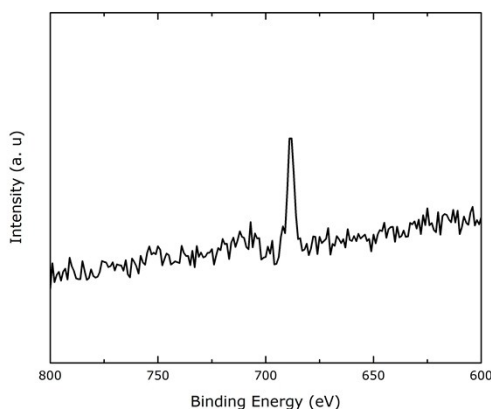


Fig. S26. F 1s XPS spectrum of MIL-101(Cr)-4F(1%).

S10. References

- [1] (a) G. Akiyama, R. Matsuda, H. Sato, M. Takata and S. Kitagawa, *Adv. Mater.*, 2011, **23**, 3294; (b) M. L. Díaz-Ramírez, E. Sánchez-González, J. R. Álvarez, G. A. González-Martínez, S. Horike, K. Kadota, K. Sumida, E. González-Zamora, M.-A. Springuel-Huet, A. Gutiérrez-Alejandre, V. Jancik, S. Furukawa, S. Kitagawa, I. A. Ibarra and E. Lima, *J. Mater. Chem. A*, 2019, **7**, 15101.
- [2] S. V. Mileghem and W. M. De Borggraeve, *Org. Process Res. Dev.* 2017, **21**, 5, 785-787.
- [3] M. Lammert, S. Bernt, F. Vermoortele, D. E. de Vos and N. Stock, *Inorganic Chemistry*, 2013, **52**, 8521–8528.
- [4] B. Qi, Y. Liu, T. Zheng, Q. Gao, X. Yan, Y. Jiao, Y. Yang, *Journal of Solid-State Chemistry*, 2018, **258**, 49-55.
- [5] F.Y. Zhang, S. G. Advani, A.K. Prasad, M.E. Boggs, S. P. Sullivan and T. P. Beebe, *Electrochim. Acta*, 2009, **54**, 4025.